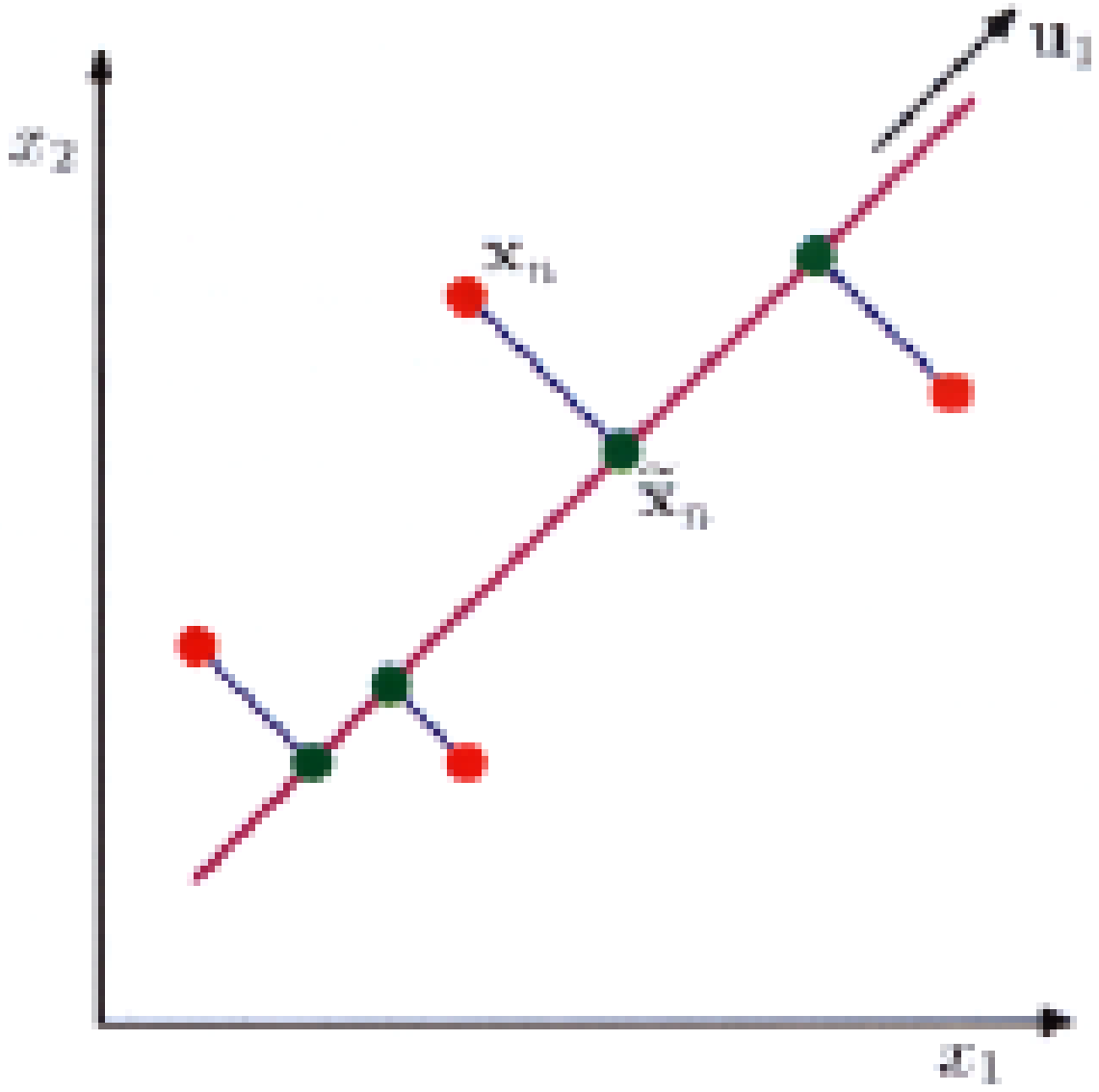
u_1
x_2
x_n
$\bar{x}_n$
x_1

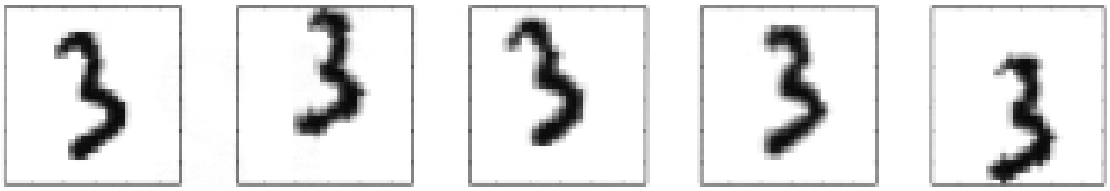

Figure 12.1 A synthetic data set obtained by taking one of the off-line digit images and creating multiple copies in each of which the digit has undergone a random displacement and rotation within some larger image field. The resulting images each have $100 \times 100 = 10,000$ pixels.

Figure 12.3 The mean vector $\bar{\mathbf{x}}$ along with the first four PCA eigenvectors $\mathbf{u}_1, \ldots, \mathbf{u}_4$ for the off-line digits data set, together with the corresponding eigenvalues.

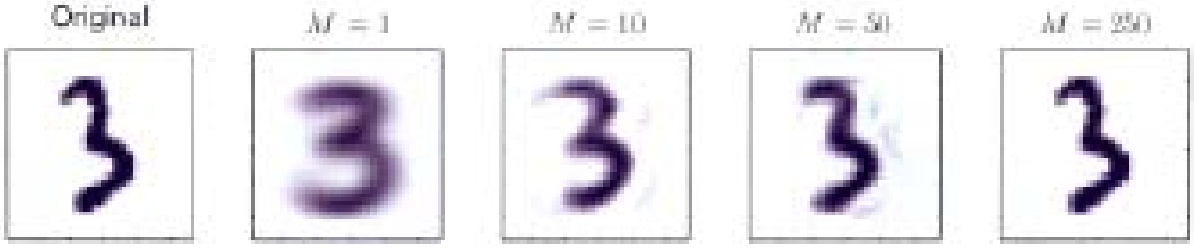

Figure 12.5 An original example from the off-line digits data set together with its PCA reconstructions obtained by retaining M principal components for various values of M. As M increases the reconstruction becomes more accurate and would become perfect when $M = D = 28 \times 28 = 784$.

Figure A.2 The three geometrical configurations of the oil, water, and gas phases used to generate the oil-flow data set. For each configuration, the pro-portions of the three phases can vary.

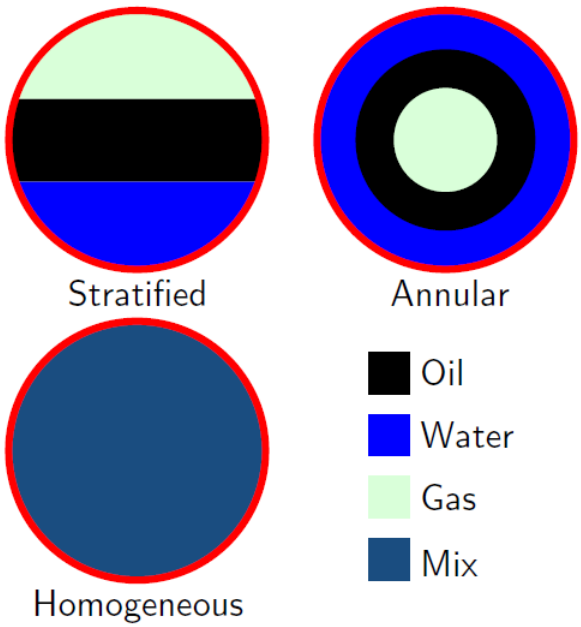

Figure A.3 Cross section of the pipe showing the arrangement of the six beam lines, each of which comprises a single dual-energy gamma densitometer. Note that the vertical beams are asymmetrically arranged relative to the central axis (shown by the dotted line).

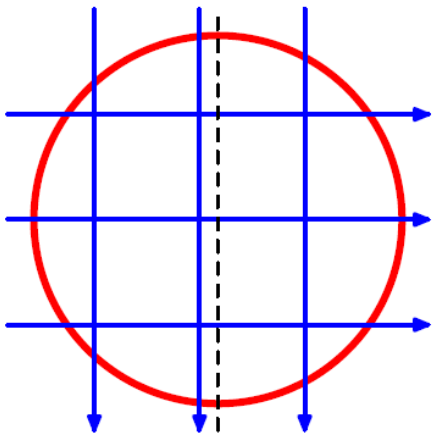

Figure 12.8 Visualization of the oil flow data set obtained by projecting the data onto the first two principal components. The red, blue, and green points correspond to the 'laminar', 'homogeneous', and 'annular' flow configurations respectively.